GLYCOSYLATION

Palladium catalysis enables cross-coupling–like S_N2-glycosylation of phenols

Li-Fan Deng[1]†, Yingwei Wang[2]†, Shiyang Xu[1], Ao Shen[1], Hangping Zhu[1], Siyu Zhang[1], Xia Zhang[1], Dawen Niu[1]*

Despite their importance in life and material sciences, the efficient construction of stereo-defined glycosides remains a challenge. Studies of carbohydrate functions would be advanced if glycosylation methods were as reliable and modular as palladium (Pd)-catalyzed cross-coupling. However, Pd-catalysis excels in forming sp^2-hybridized carbon centers whereas glycosylation mostly builds sp^3-hybridized C–O linkages. We report a glycosylation platform through Pd-catalyzed S_N2 displacement from phenols toward bench-stable, aryl-iodide–containing glycosyl sulfides. The key Pd(II) oxidative addition intermediate diverges from an arylating agent (Csp^2 electrophile) to a glycosylating agent (Csp^3 electrophile). This method inherits many merits of cross-coupling reactions, including operational simplicity and functional group tolerance. It preserves the S_N2 mechanism for various substrates and is amenable to late-stage glycosylation of commercial drugs and natural products.

The utility of glycosides in medicinal chemistry, materials, and biological science is well appreciated (*1*, *2*) but difficulties in their synthesis by glycosylation pose substantial obstacles to exploring their functions. Both reactants in glycosylation—the glycosyl donors and acceptors—are often structurally complex, and the properties of products are profoundly affected by the absolute configuration of glycosidic centers. Therefore, an ideal glycosylation method needs to simultaneously address chemo- and stereoselectivity issues, two persistent challenges in synthesis.

Glycoside synthesis has been propelled by the introduction of new donors and their activating approaches. Most reported glycosylation methods proceed under (Lewis) acid-promoted conditions, which convert glycosyl donors to (equivalents of) oxocarbenium ions for subsequent trapping by acceptors (*3*, *4*). These techniques have been the cornerstones in carbohydrate synthesis and have allowed for preparation of complex structures (*5*–*8*). However, controlling or predicting stereoselectivity remains nontrivial as the glycosylation mechanism often shifts within the S_N1/S_N2 continuum (*9*), depending on the properties of reactants and reaction parameters (*10*). Issues can also arise when labile donors or harsh activating conditions are needed, complicating reaction setup. Among the venues to overcome these obstacles, developments include the Yu group (*11*), which exploits selective gold-alkyne interactions; the Jacobsen group (*12*, *13*), which explores mild hydrogen-bond catalysis; the Miller group (*14*, *15*), which harnesses the strong Ca–F bond-forming energy; the Nguyen group (*16*) that employs Lewis base catalysis; and the Codée (*17*), Takemoto (*18*), and Loh groups (*19*), which utilize halogen-bond catalysis, and others based on transition metal catalysis (*20*, *21*). We have reported radical activation of glycosyl donors (*22*). Despite this progress, there is still a high demand for methods with a general scope to prepare stereodefined glycosides in a simple and predictable manner, which continues to fuel mechanistic and methodological advancements.

The modularity and reliability inherent in Pd-catalyzed cross-coupling reactions have made them indispensable tools in organic synthesis (*23*, *24*). If *O*-glycosylation could be as straightforward and robust as Pd-catalyzed cross coupling, the downstream exploration of glycosides would be greatly facilitated. However, Pd-catalysis is typically effective in activating and forging sp^2-hybridized carbon centers, whereas glycosidic bonds are mostly sp^3-hybridized C–O linkages. Strategies that can bridge this gap and channel the power of Pd-catalyzed cross coupling into the field of glycoside synthesis hold considerable potential. O'Doherty and others have applied Pd-catalyzed allylic substitution, followed by alkene (di)hydroxylation, for the de novo synthesis of *O*-glycosides (*25*, *26*). Here, we report a Pd-catalyzed S_N2 glycosylation method that commences with the oxidative addition (OA). The utility of this approach is showcased in a general and simple S_N2 glycosylation of phenols, a prominent challenge in *O*-glycoside synthesis.

Reaction design

General and straightforward methods for synthesizing stereodefined phenolic *O*-glycosides are highly valuable but remain nontrivial (*14*, *27*, *28*). Phenols—glycosylated or not—are abundant in both naturally occurring and man-made compounds (Fig. 1A) (*29*). Introdu… carbohydrate moieties into phenols has pr… to be an effective approach for modifying their physical and biological properties in drug discovery endeavors. Glycosylation of phenols (**3**) is complicated as they exhibit modest nucleophilicity compared with alcohols under acidic conditions (**1** to **2**; Fig. 1B). Moreover, phenols are ambident nucleophiles, potentially resulting in either *O*-glycosylated (**4**) or *C*-glycosylated products (**5**).

Pd-catalyzed cross-coupling reactions (Fig. 1C, left cycle) are usually initiated by Pd(0)-mediated OA (**6** to **7**), followed by ligand exchange (**7** to **8**) and reductive elimination (**8** to **9**) to give the desired products (here *O*-arylated phenols **9**). Recognizing the limitation of this cycle in activating/building Csp^3 centers (*30*), we designed a strategy (Fig. 1C, right cycle) that uses bench-stable, *ortho*-iodobiphenyl–substituted sulfides (*31*, *32*) **11** as glycosyl donors. The aryl iodide unit in **11** readily undergoes oxidative addition with Pd(0) catalysts, forming an OA complex **12** that acts as an effective glycosyl (Csp^3) electrophile, likely driven by its tendency to undergo Csp^2–S reductive elimination (indicated by dashed lines). Nucleophilic attack to **12** by phenoxides **10** proceeds through a clean and general S_N2 mechanism, resulting in inversion of the glycosyl center and generation of **13**.

As a result of the donor activation mechanism, this glycosylation method exhibits a notable tolerance toward functional groups and allows using unprotected glycosyl donors. No *O*-arylation side products are observed from the process (Fig. 1C), indicating that our approach directs the Pd-containing OA complex (such as **12**) to transition from an arylating agent (Csp^2) to a glycosylating agent (Csp^3), unveiling an unprecedented reactivity. The OA complex **12** behaves uniformly as an S_N2 electrophile, from fully oxygenated to fully deoxygenated donors, a rarity in carbohydrate chemistry. This method grants access to either isomer of the phenolic *O*-glycoside products in a predictable manner, many of which were previously challenging to obtain. The transformation occurs under mildly basic conditions and can be performed as easily as a Pd(0)-catalyzed cross-coupling reaction.

Reaction validation and condition optimization

Our study commenced with the model reaction between sulfide **14** or **15** and 4-methoxy phenol (**16**) to make *O*-glycoside **17** or **18** (Fig. 2). The stereoselective synthesis of 2-deoxyglycosides of phenols (e.g., **17**/**18**) has been difficult due to the lack of a C2-substituent as a stereodirecting auxiliary and the susceptibility of the 2-deoxyglycoside products to acid-promoted hydrolysis. Guided by the reaction design in Fig. 1C, we established conditions to make

[1]State Key Laboratory of Biotherapy and Cancer Center, West China Hospital, and School of Chemical Engineering, Sichuan University, Chengdu, China. [2]Department of Nuclear Medicine & Laboratory of Clinical Nuclear Medicine, West China Hospital, Sichuan University, Chengdu, China.
*Corresponding author. Email: niudawen@scu.edu.cn
†These authors contributed equally to this work.

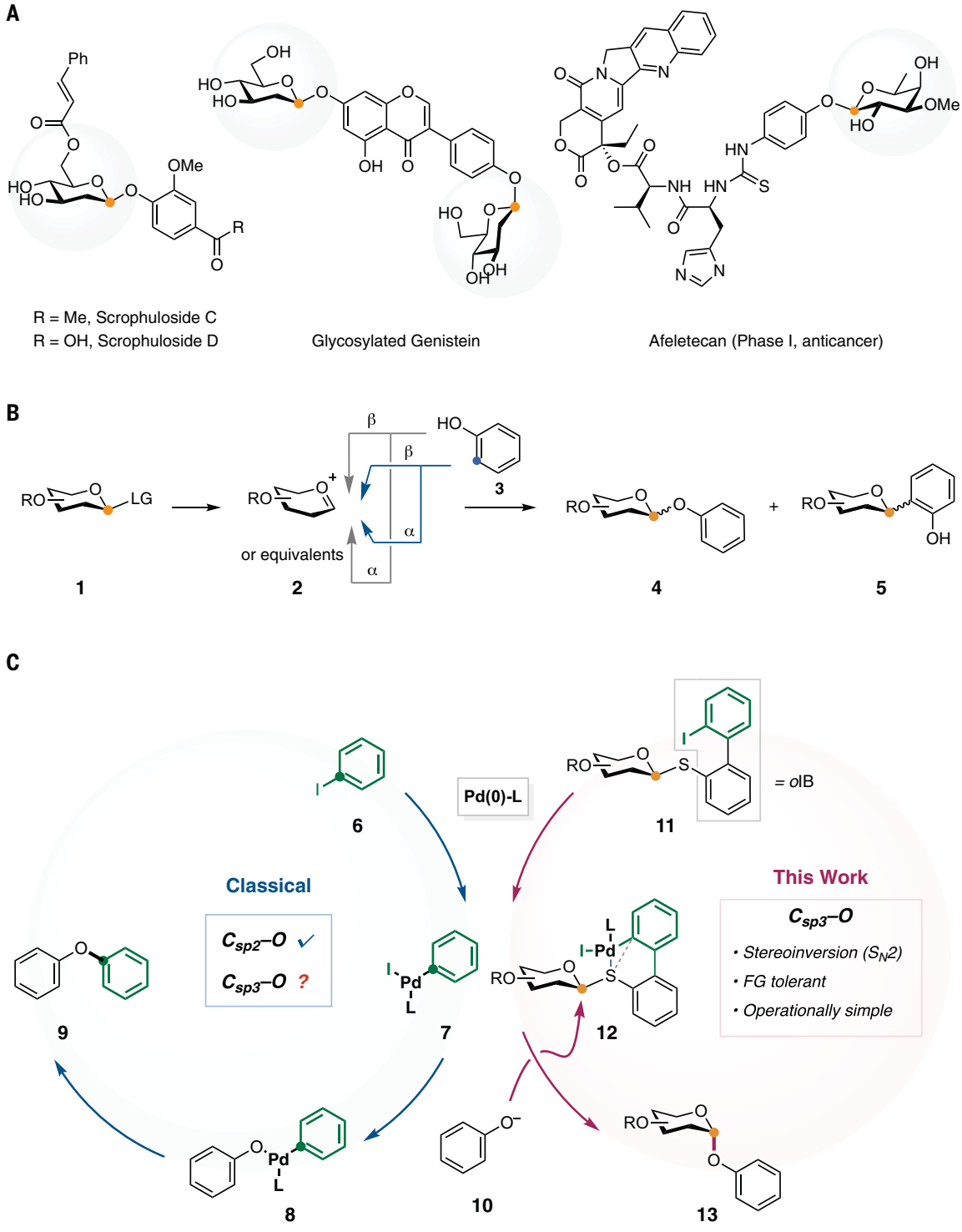

Fig. 1. Glycosylated phenols: background and synthetic approaches. (**A**) Representative examples of glycosylated phenols. (**B**) Glycosylation of phenols: challenges and limitations. (**C**) Comparison of Pd-catalyzed C–O cross-coupling and Pd-catalyzed S_N2 glycosylation (this work). FG, functional group.

O-glycosides **17**/**18** from **14**/**15** in high yields, with dibenzothiophene (**19**) formed as a byproduct. The β-*O*-glycoside **17** was obtained from the α-*S*-glycoside **14**, and α-*O*-glycoside **18** formed if β-*S*-glycoside **15** was employed. The clean inversion of the glycosidic centers in **14**/**15** suggests that this Pd-catalyzed glycosylation proceeds by means of an S_N2-type mechanism. General and operationally simple S_N2-glycosylation methods remain rare, despite their high value as tools (*12*, *34*–*36*) to access stereodefined glycosides. Even scarcer are methods that can afford both stereoisomers, as accessing the corresponding donors with defined and stable configurations is not always simple. In our case, sulfide donors (with general structure **11**) could be prepared from the corresponding 1-glycosyl thioacetates in one pot at decagram scales (see SM section 3) and stored for months without precautions to avoid air or moisture. Employing the Pd(0)-mediated OA as a donor-activating

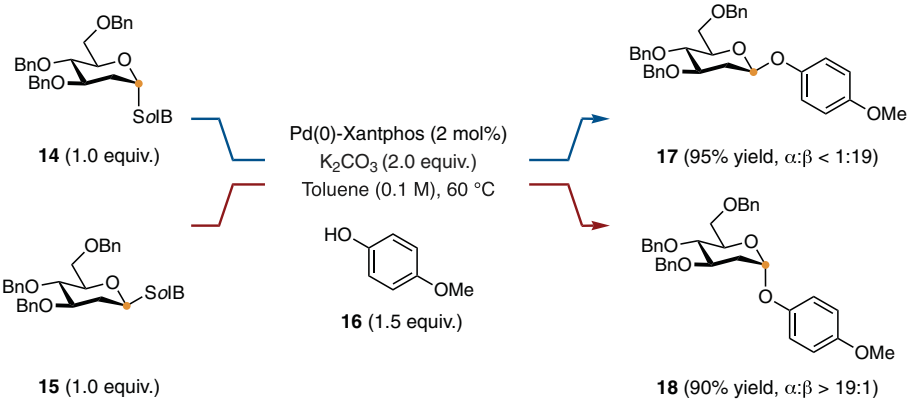

Entry	Divation from standard Conditions (with **15** used)	Conversion	Yield (α:β)
1	none	100%	92% (>19:1)
2	no Pd(0)-Xantphos	0%	0%
3	no K_2CO_3	7%	5% (>19:1)
4	Cs_2CO_3 instead of K_2CO_3	100%	94% (>19:1)
5	TEA instead of K_2CO_3	45%	20% (>19:1)
6	TMG instead of K_2CO_3	79%	54% (2:3)
7	K_2CO_3 aq.	87%	71% (9:1)
8	room temperature	21%	19% (>19:1)
9	MeCN instead of Toluene	41%	40% (1:1)
10	no XantPhos	77%	75% (>19:1)
11	NiXantPhos instead of XantPhos	100%	85% (4:1)
12	DavePhos instead of XantPhos	67%	56% (>19:1)
13	dppb instead of XantPhos	100%	90% (3:1)
14	Addition of TEMPO	100%	91% (10:1)

Ligands **Byproduct**

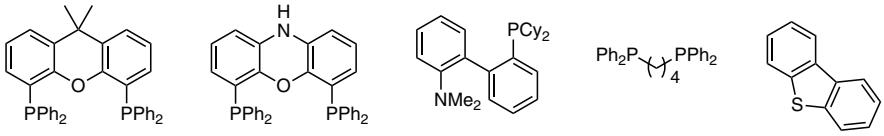

Xantphos Ni-Xantphos Davephos dppb **19**

Fig. 2. Reaction validation and condition optimization. Reactions in this table were performed at 0.05 mmol scale at 0.1 M concentration for 24 hours. Yields and conversions are determined by ^{1}H NMR analysis using 1,3,5-trimethoxy benzene as an internal standard. Diastereomeric ratios were determined by NMR analysis of crude reaction mixture. TMG, 1,1,3,3-tetramethylguanidine; TEMPO, (2,2,6,6-tetramethylpiperidin-1-yl)oxyl; Bn, benzyl.

approach, this method provides either isomer of the phenolic *O*-glycosides. The reaction proceeds at 60°C and only requires K_2CO_3 as base and a catalytic amount (2 mol%) of Pd(0) catalyst assembled from $Pd(dba)_2$ and Xantphos.

We conducted control experiments to identify factors influencing the performance of this method. Little reaction occurred in the absence of Pd(0) catalyst (entry 2) or a suitable base (entry 3). Inorganic bases K_2CO_3 (entry 1) and Cs_2CO_3 (entry 4) exhibited better effects than organic bases such as Et_3N (entry 5) and TMG (entry 6). A saturated aqueous solution of K_2CO_3 could be used (entry 7), suggesting that the reaction has a good tolerance to water. When the reaction is conducted at room temperature (roughly 25°C), the conversion is relatively low within the same time period (entry 8). The use of more polar solvents such as MeCN greatly eroded the stereochemical purity of products (entry 9). The added ligands exert pronounced effects on the reaction efficiency (entries 10 to 13), likely through modulating the properties of OA complex such as **12** in Fig. 1C. Unlike phosphine-based ligands, nitrogen-based ligands and *N*-heterocyclic carbene ligands we tried were less effective (see SM, section 4). Addition of a stoichiometric amount of TEMPO was fully tolerated, essentially excluding a radical-based mechanism (entry 14) (*22*, *37*).

Substrate scope

It is rare for a glycosylation method to hold high efficiency for a broad array of substrates as the reaction mechanism (and outcome) often varies with the reactivities of donors and acceptors (*38*–*41*). Our method accommodates diverse glycosyl units (Fig. 3), providing either of the two possible stereoisomers with high purities (**22a-m**). For example, donors bearing benzyl (**22a, 22k, 22l**), acetyl (**22b, 22f**), benzylidene (**22d**) and silyl–protecting groups (**22c, 22e**) could all be used. Various other 2-deoxypyranosyl groups (**22f-j**) were installed with similar efficiencies. Our method could be adopted to construct the more electron-rich furanosyl linkages: both isomers of 2-deoxyribosides were generated cleanly (**22k**). This method is not limited to 2-deoxy sugars, and the S_N2 mechanism operates with fully oxygenated (**22l** and **38g/h** in Fig. 4) and fully deoxygenated tetrahydropyranyl (**22m**) donors. 2-*O*-acetyl or 2-*N*-acetyl protected donors were unsuccessful, likely because of interference from these neighboring participating groups (fig. S6). Aliphatic alcohols are almost inert under the current conditions, allowing the use of unprotected glycosyl donors, as shown by examples **22g-j**. The results attest to the exceptional functional group tolerance of this OA-initiated glycosylation method. It is worth highlighting that many of the glycosyl units in Fig. 3 are deoxygenated and electron rich. To obtain the corresponding *O*-glycosides with high stereochemical purities would be tedious by conventional methods, due to dearth of suitable donors, lack of stereo-directing auxiliaries, and susceptibility of products to acid-promoted hydrolysis.

Both electron-rich (**22w, 22ae, 22ah**) and electron-deficient phenols (**22n-r**) were accommodated, with no product arising from *C*-glycosylation observed. Phenols bearing an *ortho*-substituent were competent substrates (**22u-w, 22y-z**). Functional groups such as aldehydes (**22q**), esters (**22r**), secondary amides (**22af**), nitriles (**22p**), and ketones (**22x**) were tolerated. The terminal alkene group in **22v** did not isomerize to conjugate with a phenyl ring.

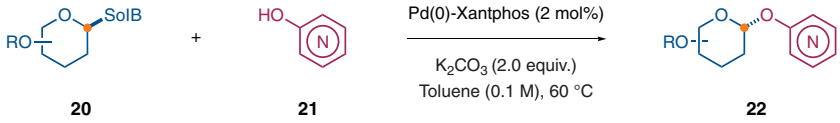

20 **21** **22**

Scope of donor, acceptor = 16 or 4-CO_2MePhOH

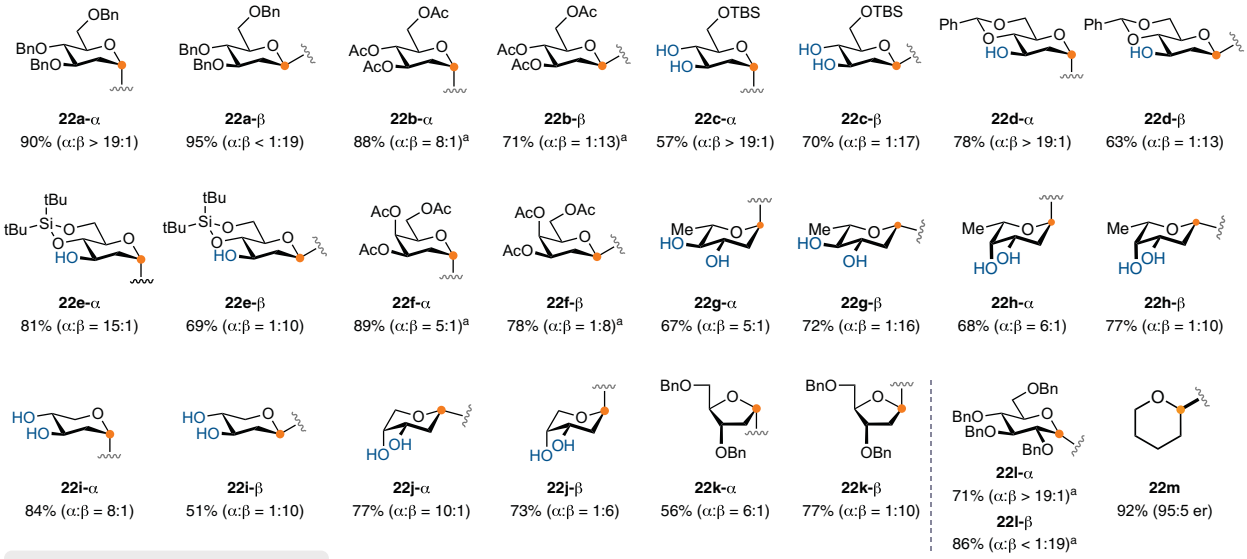

22a-α 90% (α:β > 19:1)
22a-β 95% (α:β < 1:19)
22b-α 88% (α:β = 8:1)[a]
22b-β 71% (α:β = 1:13)[a]
22c-α 57% (α:β > 19:1)
22c-β 70% (α:β = 1:17)
22d-α 78% (α:β > 19:1)
22d-β 63% (α:β = 1:13)
22e-α 81% (α:β = 15:1)
22e-β 69% (α:β = 1:10)
22f-α 89% (α:β = 5:1)[a]
22f-β 78% (α:β = 1:8)[a]
22g-α 67% (α:β = 5:1)
22g-β 72% (α:β = 1:16)
22h-α 68% (α:β = 6:1)
22h-β 77% (α:β = 1:10)
22i-α 84% (α:β = 8:1)
22i-β 51% (α:β = 1:10)
22j-α 77% (α:β = 10:1)
22j-β 73% (α:β = 1:6)
22k-α 56% (α:β = 6:1)
22k-β 77% (α:β = 1:10)
22l-α 71% (α:β > 19:1)[a]
22l-β 86% (α:β < 1:19)[a]
22m 92% (95:5 er)

Scope of acceptor, donor = 14/15

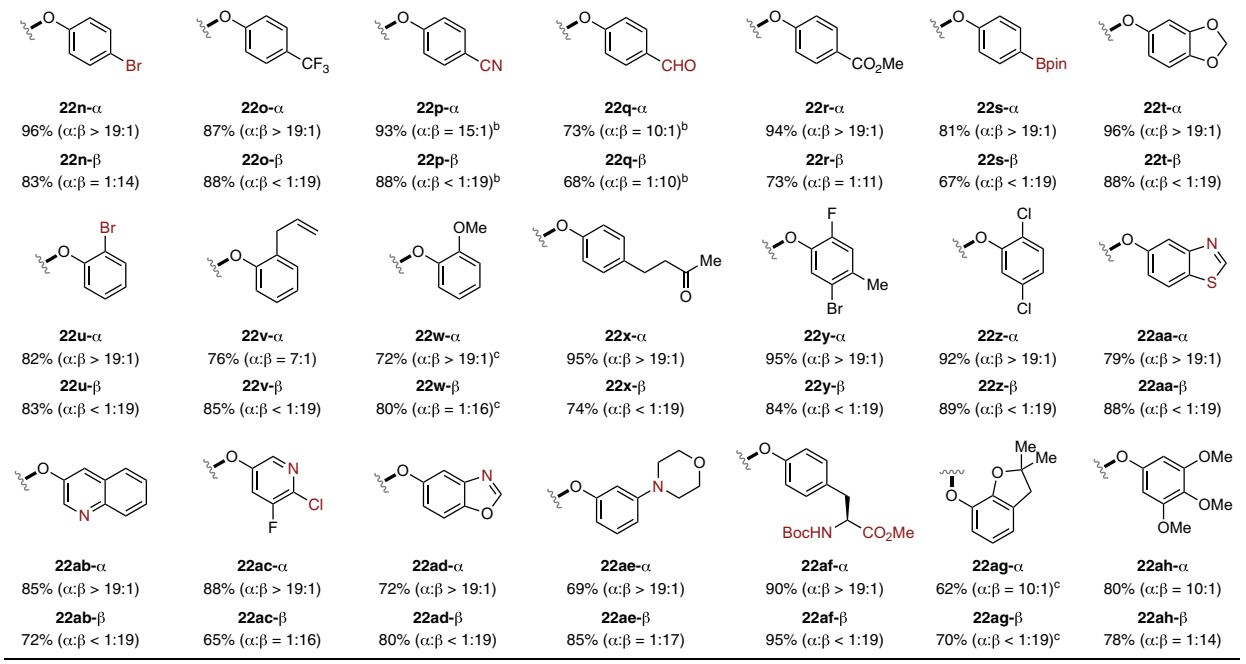

22n-α 96% (α:β > 19:1)
22n-β 83% (α:β = 1:14)
22o-α 87% (α:β > 19:1)
22o-β 88% (α:β < 1:19)
22p-α 93% (α:β = 15:1)[b]
22p-β 88% (α:β < 1:19)[b]
22q-α 73% (α:β = 10:1)[b]
22q-β 68% (α:β = 1:10)[b]
22r-α 94% (α:β > 19:1)
22r-β 73% (α:β = 1:11)
22s-α 81% (α:β > 19:1)
22s-β 67% (α:β < 1:19)
22t-α 96% (α:β > 19:1)
22t-β 88% (α:β < 1:19)
22u-α 82% (α:β > 19:1)
22u-β 83% (α:β < 1:19)
22v-α 76% (α:β = 7:1)
22v-β 85% (α:β < 1:19)
22w-α 72% (α:β > 19:1)[c]
22w-β 80% (α:β = 1:16)[c]
22x-α 95% (α:β > 19:1)
22x-β 74% (α:β < 1:19)
22y-α 95% (α:β > 19:1)
22y-β 84% (α:β < 1:19)
22z-α 92% (α:β > 19:1)
22z-β 89% (α:β < 1:19)
22aa-α 79% (α:β > 19:1)
22aa-β 88% (α:β < 1:19)
22ab-α 85% (α:β > 19:1)
22ab-β 72% (α:β < 1:19)
22ac-α 88% (α:β > 19:1)
22ac-β 65% (α:β = 1:16)
22ad-α 72% (α:β > 19:1)
22ad-β 80% (α:β < 1:19)
22ae-α 69% (α:β > 19:1)
22ae-β 85% (α:β = 1:17)
22af-α 90% (α:β > 19:1)
22af-β 95% (α:β < 1:19)
22ag-α 62% (α:β = 10:1)[c]
22ag-β 70% (α:β < 1:19)[c]
22ah-α 80% (α:β = 10:1)
22ah-β 78% (α:β = 1:14)

Fig. 3. Substrate scope. Unless otherwise noted, reactions in this table were performed at 0.1 or 0.2 mmol scale in toluene (0.1 M) for 24 hours, using $Pd(PPh_3)_4$ (2 mol%), Xantphos (4 mol%), and K_2CO_3. Isolated yields are reported. Diastereomeric ratios were determined by NMR analysis of crude reaction mixture. The [a]reaction was run at 80°C; [b]Ni-XantPhos was used instead of XantPhos; [c]Cs_2CO_3 as base. See SM, section 5 for experimental details.

Potentially chelating heterocycles including dioxolanes (**22t**), thiazoles (**22aa**), quinolines (**22ab**), pyridines (**22ac**), oxazoles (**22ad**), and morpholines (**22ae**) were incorporated. Protic hydrogen atoms in secondary amides (**22af**) were compatible. Tyrosine derivatives could be glycosylated (**22af**), and the α-stereocenter in the amino acid backbone stayed intact. Aryl bromides/chlorides (**22n, 22u, 22y-z**) did not interfere with this method, likely because the oxidative addition to aryl iodide units in donor **14** or **15** is a faster process. The remaining aryl halide groups could serve as handles for further derivatizations (see below). Particularly noteworthy is that aryl boronic esters (**22s**) survived the reaction conditions without undergoing a Suzuki-Miyaura reaction, highlighting the distinctive reactivity of our

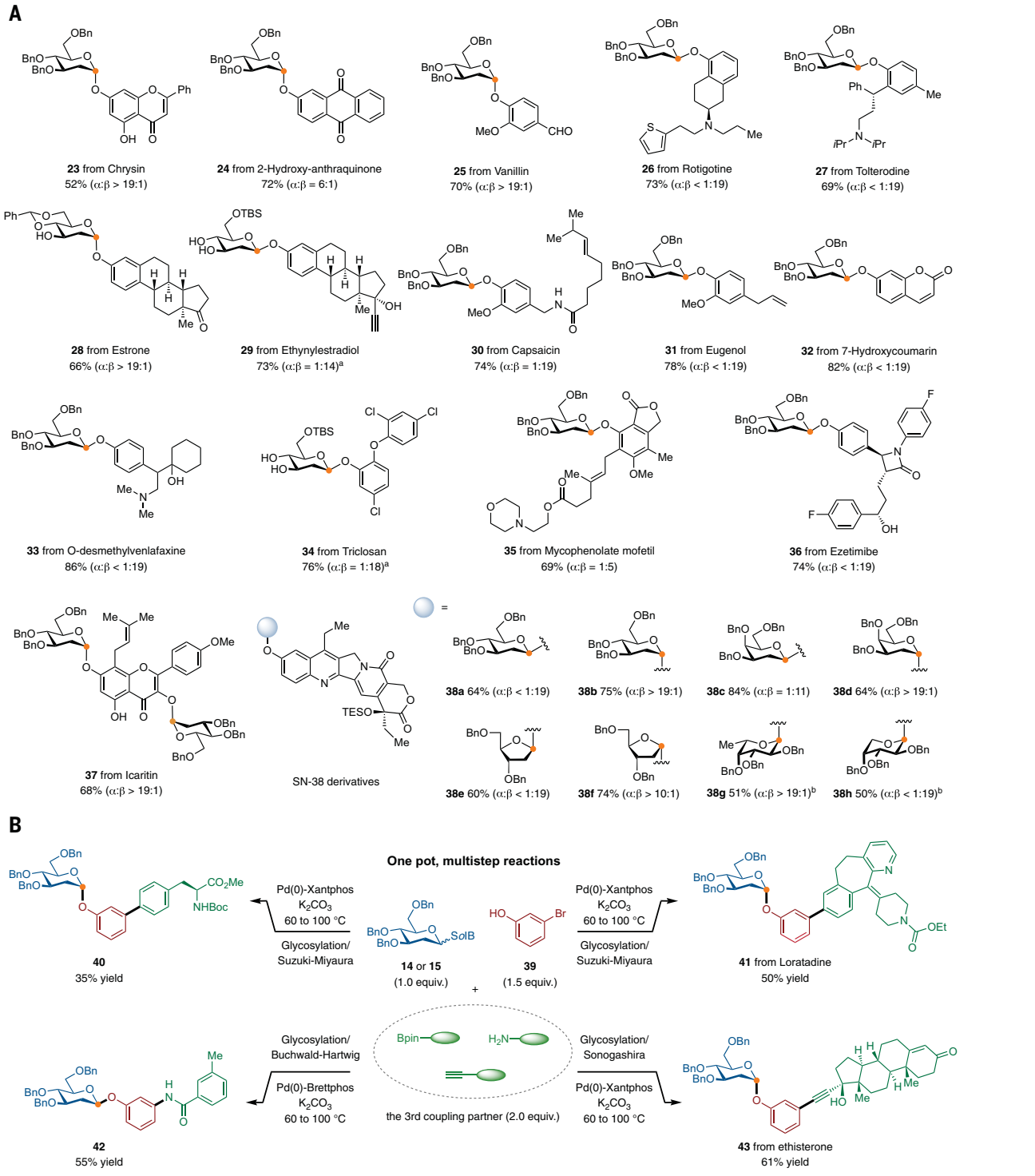

Fig. 4. Synthetic application. (**A**) Glycosylation of natural products and commercial drugs. (**B**) One-pot, multistep, multicomponent reactions. Reactions in this table were performed at 0.1 or 0.2 mmol scale in toluene (0.1 M) for 24 hours, using $Pd(PPh_3)_4$ (2 mol%), Xantphos (4 mol%), and Cs_2CO_3. Isolated yields are reported. Diastereomeric ratios were determined by NMR analysis. [a]K_2CO_3 used as base; [b]Reaction performed at 100 °C. See SM sections 6 and 7 for experimental details.

Pd(II) OA complexes (i.e., **12** in Fig. 1C) as glycosyl (Csp^3) electrophiles.

Synthetic application

To demonstrate the utility of this method, we applied it in the modification of natural products and commercial drugs (Fig. 4A). Simple phenols such as vanillin (**25**) and triclosan (**34**) were glycosylated smoothly. Internal alkene groups are accommodated, as exemplified by the formation of **30-31** and **35**. The tertiary amine groups in drug molecules may interfere with acid-promoted glycosylation methods, but show excellent compatibility with our conditions (**26-27**, **33**). Under our conditions, protection of aliphatic alcohols is unnecessary (**29**, **33**). In the case of chrysin (**23**), the C7-OH is glycosylated with high regioselectivity.

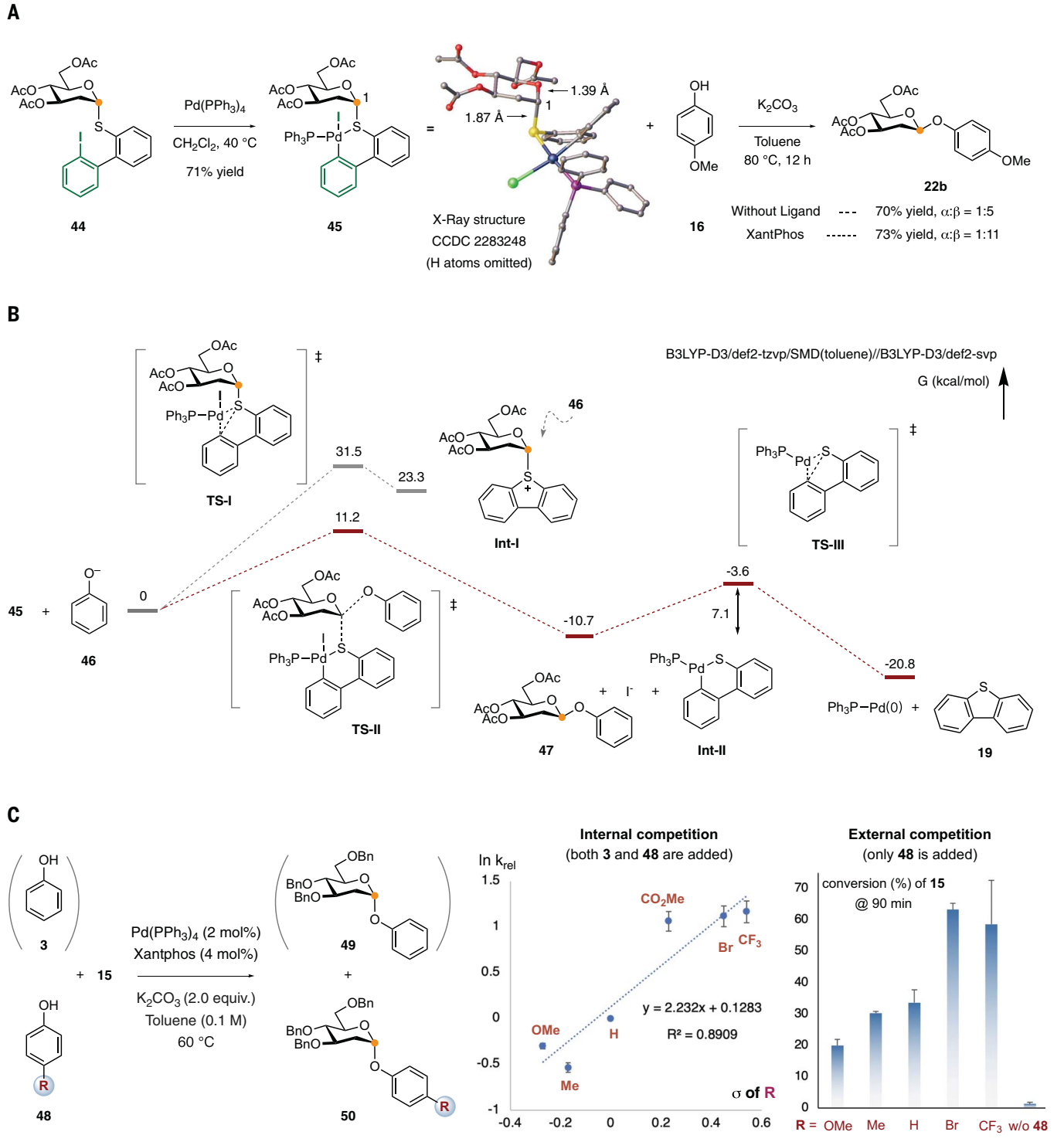

Fig. 5. Mechanistic studies. (**A**) OA complex **45**, formation, isolation, structure and reactivity. (**B**) Computed energetics for potential reaction pathways. Free energies are computed by B3LYP-D3/def2-tzvp/SMD(toluene)//B3LYP-D3/def2-svp. (**C**) Reactivity of various phenols. Procedures to determine relative rate k_{rel}: phenol (0.1 mmol), substituted phenol **48** (0.1 mmol) and glycosyl donor **15** (0.1 mmol) are allowed to react under standard conditions and stopped at ~30% conversion. k_{rel}, conversion of substituted phenol divided by conversion of phenol. The results are the average of three runs. Error bars represent standard deviations. See SM section 8 for experimental details.

For polyphenols such as icaritin (**37**), two glycosyl units can be installed at a time, both with high selectivities. Glycosylated anthraquinones are ubiquitous in nature and we show that 2-hydroxylanthraquinone is a competent substrate in our reaction (**24**). *O*-glycosylated coumarins are frequently employed as fluorescent probes for detection of glycosidases (*42*), and coumarins are glycosylated cleanly (**32**). Steriodal phenols such as estrone (**28**) and estradiol (**29**) are modified. A glycosyl unit was installed onto ezetimibe (**36**), a cholesterol absorption

inhibitor containing a sensitive β-lactam unit. SN-38 is a potent anticancer agent derived from camptothecin (*43*) but is poorly soluble in water. Conjugation with a sugar may improve the pharmacological profile of the parent molecule; see Afeletecan in Fig. 1A. We mounted an array of glycosyl units, including both C2-deoxygenated (**38a-f**) and C2-oxygenated sugars (**38g-h**), onto an SN-38 derivative (Fig. 4A).

Pd-catalyzed S_N2 glycosylation could be performed in tandem with other Pd-catalyzed cross-coupling reactions, affording carbohydrate-containing compounds by one-pot, multistep processes in which a single Pd(0)-complex catalyzes two distinct steps (Fig. 4B). Mixing glycosyl donor **14** or **15**, *m*-bromo phenol (**39**), and aryl boronic ester in one pot with a Pd(0)-catalyst and a base, the Pd-catalyzed glycosylation and the Suzuki-Miyaura coupling proceed in sequence, to give loratadine derivative **41** or *L*-tyrosine derivative **40** in useful overall yields. The glycosylation could also be merged with Buchwald-Hartwig (*44*, *45*) coupling if the ligand is switched to Brettphos (*46*) and *m*-toluamide as the third coupling partner; consecutive formation of Csp^3–O and Csp^2–N bonds delivered **42** smoothly. Lastly, a sequence composed of glycosylation/Sonogashira coupling provides ethisterone-sugar conjugate **43** in 61% overall yield. These examples illustrate selectivity of our Pd-catalyzed glycosylation and suggest a rapid approach to make glycoconjugates.

Mechanistic studies

Acetyl-protected sulfide donor **44** reacted with $Pd(PPh_3)_4$ smoothly, and the OA complex **45** could be isolated from the mixture by column chromatography (Fig. 5A). The facility of the OA step may be attributable to the sulfur atom in **44**, which could pre-coordinate with Pd(0). Complex **45** is a crystalline solid and its molecular structure was verified by x-ray crystallography. Similar to other classical Pd(II) OA complexes (*47*), the Pd center in **45** adopts a (slightly twisted) square planar configuration, with the two neutral ligands (i.e., sulfur and phosphine atoms) occupying para positions. From the solid-state structure of **45**, we noted that the C1–S bond is slightly elongated (1.83 to 1.87 Å) and the C1–O bond is shortened (1.41 to 1.39 Å) from their normal lengths (*48*), indicating buildup of a positive charge at the C1 position.

Treating **45** with 4-methoxy phenol (**16**) in the presence of K_2CO_3 afforded **22b** with decent efficiency and inverted configuration. Addition of external ligand Xantphos gave similar results. A small amount of **45** (2 mol%) could catalyze the reaction between **44** and **16** to form **22b**. These results support **45** as a reactive intermediate in our process.

We next performed DFT calculations (B3LYP-D3/def2-tzvp/SMD(toluene)//B3LYP-D3/def2-svp) employing **45** and phenoxide **46** (or cesium phenoxide, see SM section 9) as model substrates (Fig. 5B). Two potential pathways were examined: In principle, reductive elimination of C–S bond in **45** to yield sulfonium **Int-I** (by means of **TS-I**), followed by phenoxide attack from **46** could afford glycoside **47**. Alternatively, direct attack of phenoxide **46** toward **45** by means of **TS-II**, followed by reductive elimination of the C–S bond (*45*) in **Int-II** would provide **47** as well, affording **19** as a byproduct and regenerating Pd(0) catalyst. Upon comparing the free energies of species **TS-I** and **TS-II** (note: with different charge states), we observed that the pathway through **TS-II** exhibits lower barriers. Presumably, coordination of the sulfur atom to the Pd center polarized the C–S bond in **45** and made it electrophilic enough toward phenoxide attack. We also considered a scenario where the iodine anion dissociates early from **45** before S_N2 displacement by **46** (see SM, section 9).

We also compared the relative reactivities of various phenols bearing different para-substituents (**48**) in our glycosylation reaction (Fig. 5C). In internal competition experiments, those with electron-withdrawing substituents (*49*) react at faster rates, presumably because they are more easily deprotonated under basic conditions. By external competition experiments, we found that the turnover frequency, as inferred from the conversion of **15**, increases with the electron-withdrawing ability of the para-substituent. The absence of phenol **48** resulted in essentially no reaction. These results indicate the involvement of phenoxide nucleophiles in the turnover-determining step and in turn lend some further support for the pathway through **TS-II**. Although additional experiments are warranted to elucidate mechanistic details, the ability of Pd-containing OA complex to serve as a glycosyl (Csp^3) electrophile was quite general (see examples in Figs. 3 and 4).

Conclusions

We developed a strategy that exploits Pd(0)-mediated oxidative addition—the initial step in classical cross-coupling reactions—as a tool to activate glycosyl donors. The key to this success was the use of aryl iodide-containing glycosyl sulfides as donors, which upon reaction with Pd(0)-catalysts furnished Pd(II)-containing OA complexes that act as glycosyl (Csp^3) electrophiles. The following glycosidic bond-forming stage caused clean inversion of the glycosyl centers in donors, and either stereoisomer could be obtained in a predictable manner. This approach enabled a general method for S_N2-glycosylation of phenols, allowing for the synthesis of phenolic *O*-glycosides that were previously challenging to access.

The mechanism grants this reaction operational simplicity and functional group tolerance. No acid or cryogenic conditions are required, and the reaction can be set up similarly to other Pd-catalyzed C–O cross-coupling reactions. Moreover, the method is amenable to late-stage glycosylation of a wide range of commercial drugs and natural products. The generality and mildness of the method is further showcased in several one-pot, multistep, multicomponent reactions. We anticipate that this study will bring opportunities in Pd-mediated glycosylation reactions, enabling advancements in carbohydrate synthesis and its application in various fields.

REFERENCES AND NOTES

1. A. Varki *et al*., *Essentials of Glycobiology* (Cold Spring Harbor, 2022), ed. 4
2. J. J. Barchi, *Comprehensive Glycoscience: From Chemistry to Systems Biology* (Elsevier, 2021), ed. 2
3. A. V. Demchenko, *Handbook of Chemical Glycosylation*. (Wiley, 2008).
4. D. B. Werz, S. Vidal, *Modern Synthetic Methods in Carbohydrate Chemistry: From Monosaccharides to Complex Glycoconjugates* (Wiley, 2014).
5. S. J. Danishefsky, Y.-K. Shue, M. N. Chang, C.-H. Wong, *Acc. Chem. Res.* **48**, 643–652 (2015).
6. X. Zou *et al*., *J. Am. Chem. Soc.* **140**, 3120–3127 (2018).
7. X. Xiao *et al*., *J. Am. Chem. Soc.* **142**, 5498–5503 (2020).
8. W. Yao *et al*., *Nat. Synth.* **1**, 854–863 (2022).
9. P. O. Adero, H. Amarasekara, P. Wen, L. Bohé, D. Crich, *Chem. Rev.* **118**, 8242–8284 (2018).
10. S. Chatterjee, S. Moon, F. Hentschel, K. Gilmore, P. H. Seeberger, *J. Am. Chem. Soc.* **140**, 11942–11953 (2018).
11. B. Yu, *Acc. Chem. Res.* **51**, 507–516 (2018).
12. Y. Park *et al*., *Science* **355**, 162–166 (2017).
13. Q. Li, S. M. Levi, C. C. Wagen, A. E. Wendlandt, E. N. Jacobsen, *Nature* **608**, 74–79 (2022).
14. T. J. Wadzinski *et al*., *Nat. Chem.* **10**, 644–652 (2018).
15. G. Pelletier, A. Zwicker, C. L. Allen, A. Schepartz, S. J. Miller, *J. Am. Chem. Soc.* **138**, 3175–3182 (2016).
16. J. Li, H. M. Nguyen, *Acc. Chem. Res.* **55**, 3738–3751 (2022).
17. R. Castelli *et al*., *Chem. Asian J.* **9**, 2095–2098 (2014).
18. Y. Kobayashi, Y. Nakatsuji, S. Li, S. Tsuzuki, Y. Takemoto, *Angew. Chem. Int. Ed.* **57**, 3646–3650 (2018).
19. C. C. J. Loh, *Nat. Rev. Chem.* **5**, 792–815 (2021).
20. M. J. McKay, H. M. Nguyen, *ACS Catal.* **2**, 1563–1595 (2012).
21. X. Li, J. Zhu, *Eur. J. Org. Chem.* **2016**, 4724–4767 (2016).
22. W. Shang, D. Niu, *Acc. Chem. Res.* **56**, 2473–2488 (2023).
23. C. C. C. Johansson Seechurn, M. O. Kitching, T. J. Colacot, V. Snieckus, *Angew. Chem. Int. Ed.* **51**, 5062–5085 (2012).
24. K. C. Nicolaou, P. G. Bulger, D. Sarlah, *Angew. Chem. Int. Ed.* **44**, 4442–4489 (2005).
25. D. Ray, G. A. O'Doherty, in *Protecting Groups: Strategies and Applications in Carbohydrate Chemistry*, Edited by S. Vidal (Wiley, 2019), Ch. 9.
26. R. S. Babu, G. A. O'Doherty, *J. Am. Chem. Soc.* **125**, 12406–12407 (2003).
27. M. Jacobsson, J. Malmberg, U. Ellervik, *Carbohydr. Res.* **341**, 1266–1281 (2006).
28. Y. Li, H. Mo, G. Lian, B. Yu, *Carbohydr. Res.* **363**, 14–22 (2012).
29. Z. Rappoport, *The Chemistry of Phenols* (Wiley, 2003).
30. N. Kambe, T. Iwasaki, J. Terao, *Chem. Soc. Rev.* **40**, 4937–4947 (2011).
31. T. Ooi, M. Furuya, D. Sakai, K. Maruoka, *Adv. Synth. Catal.* **343**, 166–168 (2001).
32. Y. Wang, L.-F. Deng, X. Zhang, Z.-D. Mou, D. Niu, *Angew. Chem. Int. Ed.* **60**, 2155–2159 (2021).
33. C. S. Bennett, M. C. Galan, *Chem. Rev.* **118**, 7931–7985 (2018).
34. X. Ma *et al*., *J. Am. Chem. Soc.* **143**, 11908–11913 (2021).
35. J. P. Issa, C. S. Bennett, *J. Am. Chem. Soc.* **136**, 5740–5744 (2014).
36. M. H. Zhuo, D. J. Wilbur, E. E. Kwan, C. S. Bennett, *J. Am. Chem. Soc.* **141**, 16743–16754 (2019).
37. Y. Jiang, Y. Zhang, B. C. Lee, M. J. Koh, *Angew. Chem. Int. Ed.* **62**, e202305138 (2023).
38. H. D. Premathilake, A. V. Demchenko, *Top. Curr. Chem.* **301**, 189–221 (2011).
39. K. M. Koeller, C. H. Wong, *Chem. Rev.* **100**, 4465–4494 (2000).

40. C. W. Chang *et al*., *Angew. Chem. Int. Ed.* **60**, 12413–12423 (2021).
41. S. van der Vorm *et al*., *Angew. Chem. Int. Ed.* **57**, 8240–8244 (2018).
42. B. Thomas *et al*., *Chem. Soc. Rev.* **49**, 593–641 (2020).
43. F. Li, T. Jiang, Q. Li, X. Ling, *Am. J. Cancer Res.* **7**, 2350–2394 (2017).
44. P. Ruiz-Castillo, S. L. Buchwald, *Chem. Rev.* **116**, 12564–12649 (2016).
45. J. F. Hartwig, *Acc. Chem. Res.* **41**, 1534–1544 (2008).
46. B. P. Fors, D. A. Watson, M. R. Biscoe, S. L. Buchwald, *J. Am. Chem. Soc.* **130**, 13552–13554 (2008).
47. C. Bolm, K. Wenz, G. Raabe, *J. Organomet. Chem.* **662**, 23–33 (2002).
48. H. Liu *et al*., *J. Am. Chem. Soc.* **145**, 3682–3695 (2023).
49. C. Hansch, A. Leo, R. W. Taft, *Chem. Rev.* **91**, 165–195 (1991).

ACKNOWLEDGMENTS

We acknowledge P. Yu (SusTEC) for helpful discussions and computational resources. We also thank J. Yang (SCU) for helpful suggestions. **Funding:** D.N. is supported by National Natural Science Foundation of China (T2221004 and 21922106). **Author contributions:** D.N. conceived the idea, guided the project, and wrote the manuscript with feedbacks from other authors. L.-F.D. and Y.W. made the initial observations and analyzed the results. L.-F.D., Y.W., A.S., S.Z., and H.Z. explored substrate scope. L.-F.D. and Y.W. performed the mechanistic studies. Under the guidance of X.Z. and D.N, S.X. performed DFT calculations. **Competing interests:** The authors declare no competing interests. **Data and materials availability:** Crystallographic data for compound **45** are available from the Cambridge Crystallographic Data Center under reference number CCDC 2283248. All other data discussed in this paper are available in the main text or Supplementary Materials.

SUPPLEMENTARY MATERIALS

science.org/doi/10.1126/science.adk1111
Materials and Methods
Supplementary Text
Figs. S1 to S9
References (*50*–*63*)

Submitted 4 August 2023; accepted 24 October 2023
10.1126/science.adk1111

Palladium catalysis enables cross-coupling–like S_N2-glycosylation of phenols

Li-Fan Deng, Yingwei Wang, Shiyang Xu, Ao Shen, Hangping Zhu, Siyu Zhang, Xia Zhang, and Dawen Niu

Science **382** (6673), . DOI: 10.1126/science.adk1111

Editor's summary

Glycosylations are an important feature of many natural products, but methods to install sugars can suffer from limitations on stereospecificity because many reactions proceed through an oxocarbenium intermediate in which stereochemistry is lost. Deng *et al*. developed a versatile palladium-catalyzed reaction for the glycosylation of phenols that resembles palladium-catalyzed aryl carbon–oxygen cross-coupling reactions. Palladium oxidative addition to an easily prepared ortho-iodobiphenyl S-glycoside yields a complex that reacts with a wide range of phenolates through a S_N2 mechanism to afford the glycosylated phenols with inversion of stereochemistry. This reaction works well with, but it is not limited to, 2-deoxy sugars and can be performed in one pot with other palladium-catalyzed cross-couplings to yield complex O-glycosides. —Michael A. Funk